

**CORRECTING BEAM MONITOR & DIFFRACTION DATA  
FOR CHOPPED DELAYED NEUTRON BACKGROUNDS**

John M. Carpenter  
Intense Pulsed Neutron Source, Argonne National Laboratory  
9700 South Cass Avenue, Argonne, IL 60439

David F. R. Mildner  
Center for Analytical Chemistry  
National Institute of Standards and Technology  
Gaithersburg, MD 20899

James W. Richardson, Jr.  
and

William C. Dimm<sup>a</sup>  
Intense Pulsed Neutron Source, Argonne National Laboratory  
9700 South Cass Avenue, Argonne, IL 60439

<sup>a</sup>Present address: Department of Physics, Cornell University, Ithaca, NY

ABSTRACT

Delayed neutron choppers in pulsed source neutron beams serve to reduce the background caused by delayed neutrons in pulsed source instruments. We analyze the effect of a drum chopper placed in an incident pulsed beam which contains delayed neutrons and compute its influence on the detector counting rate. Expressions are found for the time and wavelength dependence of the counting rates for both prompt and delayed neutrons, in both monitor and scattered neutron detectors. On the basis of these results, we suggest an exact, random-phasing method for determining the delayed neutron background for use in measuring the delayed neutron counting rate, and propose a rapidly convergent iterative scheme for computing the correction from normally measured data. We report measurements which confirm the analysis.

**I. INTRODUCTION**

The  $^{235}\text{U}$  enriched booster target provides enhanced neutron fluxes for the IPNS spectrometers<sup>1</sup>. Accompanying the higher pulse intensity is a relatively greater background of delayed neutrons. Methods are needed for describing, assessing and suppressing these backgrounds and applying corrections if necessary.

In order to reduce the delayed neutron backgrounds, drum choppers have been introduced in the incident beam for both SEPD (total flight path length 15.5 meters) and GPPD (21.5 meters)<sup>2</sup>. Figure 1 illustrates the arrangement. These choppers are hollow aluminum drums of 40 cm diameter spinning on a vertical axis, covered with epoxy-boron carbide of 1 cm thickness and 10.5 cm height. They have

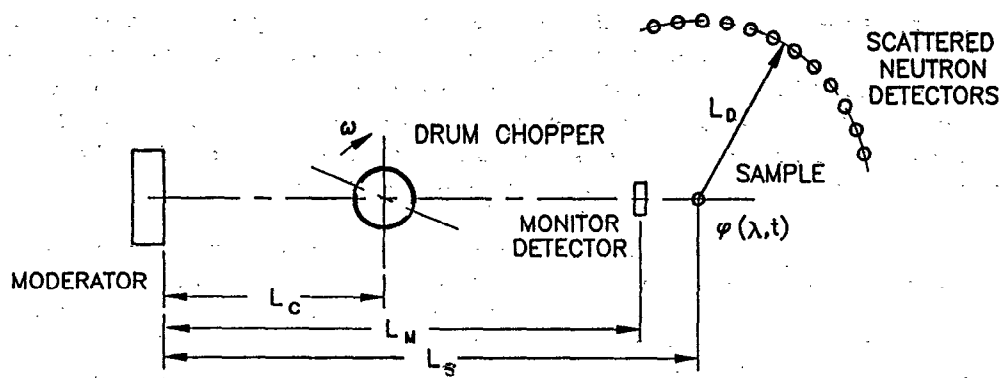


Figure 1. A schematic diagram of a source (moderator) and a drum chopper a distance  $L_C$  downstream. The source emits delayed neutrons at a steady rate and also prompt neutrons in periodic, short pulses.  $\phi(\lambda, t)$ , the flux per unit wavelength at time  $t$ , is to be determined at a point  $L$  away from the source.

symmetrically placed openings (subtending opening angles measured from the center of  $81.8^\circ$  in SEPD, and  $60.7^\circ$  in GPPD) to allow the passage of the beam. They normally rotate at 15 Hz, driven by hysteresis synchronous motors synchronized at half the frequency of the pulsed source itself and opening twice per revolution. Both choppers are located  $L_C = 6.01$  meters from the source (moderator). Appropriately phased, the drum choppers do not significantly affect the transmission of the pulsed beam in the desired wavelength range. Figure 2a is a diagram of the time of arrival of neutrons of different wavelengths vs. distance. Figure 2b shows the corresponding scattered neutron detector counting rate.

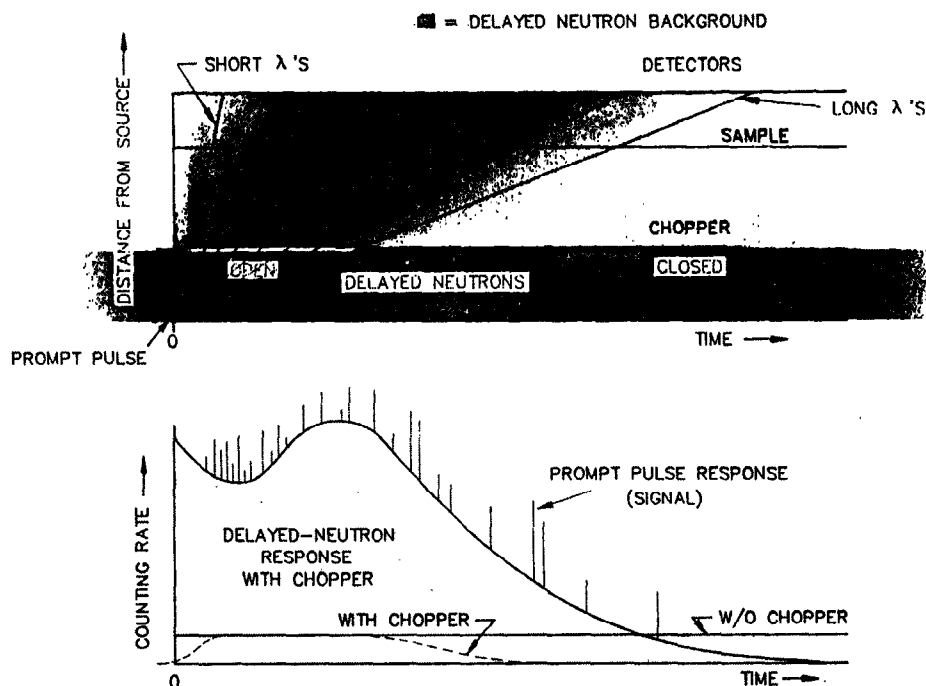


Figure 2a. Time vs. distance diagram ("neutron time schedule") showing the arrival of neutrons from the prompt pulse and of delayed neutrons. In the

absence of the delayed neutron chopper, delayed neutrons arrive at a constant rate. The chopper, shown as either closed (black bar) or open (white), modulates the delayed neutrons, and is phased to reduce the delayed neutron counting rate in the time range when the prompt neutron counting rate is low. The density of shading represents the intensity of delayed neutrons. b. The counting rate distribution corresponding to 2a., showing the prompt response with Bragg peaks, and the delayed neutron counting rate with and without the chopper.

The transmission characteristics and pulse shape of the drum chopper depend on the neutron wavelength, the frequency of rotation of the chopper, the diameter of the chopper, the width of the chopper slot and the width of the incident beam. We define a transmission probability for the chopper  $P_C(\lambda, t; \alpha_0)$ , that is, the probability that a neutron of wavelength  $\lambda$  which crosses the chopper axis at time  $t$  is transmitted through the chopper, where  $\alpha_0$  is the phase angle of the chopper at the time of origin of the pulsed beam. In reference (3) we provide full details of the calculation of this probability. Figures 3 and 4 illustrate the transmission probability  $P_C(\lambda, t; \alpha_0) = P_C(\lambda, t - \alpha_0/\omega; 0)$  for the SEPD and GPPD choppers, respectively.

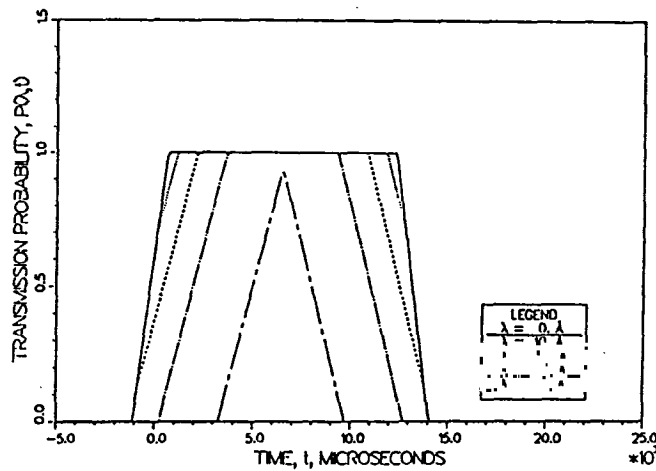


Figure 3. The transmission probability  $P_C(\lambda, t; \alpha_0)$  for the SEPD delayed neutron chopper. The nominal opening time  $t_0 = \alpha_0/\omega = 6500 \mu\text{sec}$ .

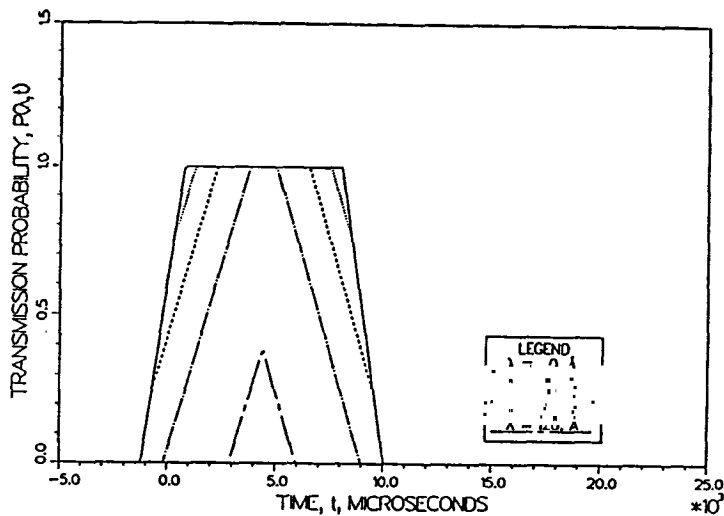


Figure 4. The transmission probability  $P_C(\lambda, t; \alpha_0)$  for the GPPD delayed neutron chopper. The nominal opening time  $t_0 = \alpha_0/\omega = 4400 \mu\text{sec}$ .

In this paper, we derive expressions for the counting rates in both the monitor and the scattered neutron detectors for both the prompt pulse and the delayed neutrons in terms of the chopper transmission probability function. We show that a random phase average counting rate, measured by running the chopper asynchronously with the pulsed source, is directly related to the delayed neutron counting rate. We introduce a rapidly convergent iterative method for calculating the delayed neutron correction from normally measured data. We report measurements of the delayed neutron background taken on two IPNS diffractometers with an incoherently scattering sample, illustrating the random phase operation and the iterative correction calculation.

## II. DETECTOR COUNTING RATE

Consider the neutron flux at a distance  $L$  from the moderator in a generalized diffraction instrument on a pulsed source, as represented in Figure 1. The flux per unit wavelength at a point a distance  $L$  from the moderator and at a time  $t$  is given by

$$\begin{aligned} \phi(\lambda, t) &= (1/L^2) \iint dt' dt'' i(\lambda, t') P_C(\lambda, t''; \alpha_0) \delta(t-t'-L/v) \delta(t''-t'-L_C/v), \\ &= (1/L^2) i(\lambda, t-L/v) P_C(\lambda, t-(L-L_C)/v; \alpha_0) \end{aligned} \quad (1)$$

where  $i(\lambda, t')$  is the beam current leaving the moderator per unit wavelength at time  $t'$  after one source pulse. The  $\delta$ -functions relate the times, distances and neutron speeds at the measurement point ( $t$ ,  $L$  and  $v$ ) and at the chopper ( $t''$ ,  $L_C$  and  $v$ ) relative to the moderator ( $t'$ ,  $0$ ,  $v$ ). Throughout,  $\lambda = (h/m)/v$ ;  $h/m = 3955.41$  Å-m/sec. The beam current is composed of a prompt pulse at the time  $t'=0$  from the moderator, and a delayed fraction  $\epsilon$  of neutrons which is assumed to be constant in time and is a known, intrinsic parameter of the source. It is reasonable to assume that the spectral distribution of the delayed neutrons is identical with that of the prompt neutrons. Thus  $i(\lambda, t')$  is related to the time-averaged beam current  $\bar{I}(\lambda)$  per unit wavelength per unit time by

$$i(\lambda, t') = \bar{I}(\lambda) [(1 - \epsilon)\delta(t')/f + \epsilon], \quad (2)$$

where  $f$  is the source pulsing frequency.

The counting rate at time  $t$  in a monitor detector in the beam is given by

$$C_M(t) = \int d\lambda \phi(\lambda, t) A_M \eta_M(\lambda), \quad (3)$$

where  $\phi(\lambda, t)$  is the neutron flux at the monitor detector at a distance  $L_M$  from the moderator.  $A_M$  is the area of the beam at the monitor and  $\eta_M(\lambda)$  is the monitor efficiency, assumed to be time-independent. The counting rate at time  $t$  in a neutron detector at a scattering angle  $\theta$  in a diffraction measurement is similarly

$$C_D(t) = \iint d\lambda du \phi(\lambda, u) \delta(t-u-L_D/v) N d\sigma/d\Omega(\lambda, \theta) \Delta\Omega_D \eta_D(\lambda), \quad (4)$$

where  $\phi(\lambda, u)$  is the neutron flux per unit wavelength at the sample, at a distance  $L_S$  from the moderator, at time  $u$ .  $N d\sigma/d\Omega(\lambda, \theta)$  the sample (assumed elastic) scattering cross section.  $L_D$  is the distance from the sample to the detector,  $\Delta\Omega_D$  is the solid angle subtended by the detector and  $\eta_D(\lambda)$  is the detector efficiency.

For the present purposes, we represent the counting rates in both the monitor and the scattered neutron detectors in one generalized expression for the counting rate, which together with (1) and (2) gives results identical in form, which is

$$C(t) = \int d\lambda F(\lambda) [(1-\epsilon) \delta(t-d/v)/f + \epsilon] P_C(\lambda, t-(d-L_C)/v; \alpha_0), \quad (5)$$

where

$$F(\lambda) = \begin{cases} \bar{I}(\lambda) A_M \eta_M(\lambda) / L_M^2 & \text{for the monitor measurement} \\ \bar{I}(\lambda) N \, d\sigma/d\Omega(\lambda, \theta) \Delta\Omega_D \eta_D(\lambda) / L_S^2 & \text{for the scattering measurement,} \end{cases} \quad (6)$$

and  $d$  is the distance from moderator to monitor ( $L_M$ ) or detector ( $L_S + L_D$ ) for each measurement. The first term in (5) is the prompt pulse response, the second term is the delayed neutron background, which is a function of the time on account of the presence of the drum chopper, and depends on  $\partial\sigma/\partial\Omega(\lambda, \theta)$ .

The prompt pulse response is

$$\begin{aligned} C_p(t) &= (1-\epsilon)/f \int d\lambda F(\lambda) \delta(t-d/v) P_C(\lambda, t-(d-L_C)/v-\alpha_0/\omega; 0), \\ &= [(1-\epsilon)/f] (h/md) F(\lambda_t) P_C(\lambda_t, L_C t/d-\alpha_0/\omega; 0) \end{aligned} \quad (7)$$

where  $\lambda_t = (h/m) t/d$ , and the delayed neutron response is

$$C_d(t) = \epsilon \int d\lambda F(\lambda) P_C(\lambda, t-(d-L_C)/v-\alpha_0/\omega; 0). \quad (8)$$

Crawford <sup>(4)</sup> has analyzed this same problem using Monte Carlo techniques. The present analytical treatment is appropriate for use in correcting data; the Monte Carlo simulation provides greater insight into "grayness" effects.

### III. RANDOM PHASE METHOD FOR DETERMINING DELAYED NEUTRON BACKGROUND

The method proposed here for measuring the delayed neutron response  $C_d(t)$  rests upon using the prompt neutrons as a continuous source equivalent to the delayed neutrons. This can be accomplished by operating the chopper very near its normal frequency, but in random phase relative to the source pulse, and analyzing the counting rate as a function of time  $t_c$  measured from a time-reference signal derived from the chopper. All phases of the chopper relative to the source are therefore uniformly sampled in the measurement, and both the constant delayed neutron part and the average prompt part accumulate identically as steady sources. (The IPNS delayed neutron chopper drive systems can operate in this mode). Then the random phase counting rate is just proportional to the delayed neutron counting rate in normal operation, with the time scale shifted by an amount equal to the time between the source pulse and the chopper time reference pulse,

$$C_d(t) = \frac{\epsilon \langle C'(t-\alpha_0/\omega) \rangle}{\left( \frac{\omega(1-\epsilon)}{\pi f} + \epsilon \right)}. \quad (9)$$

Only the delayed neutron fraction  $\epsilon$  and the phase angle (ignoring any small error)  $\alpha_0$  need to be known independently to enable  $C_d(t)$  to be determined.  $\epsilon$  follows easily from a separate measurement, and has already been measured<sup>5</sup> for the IPNS booster target, with the result  $\epsilon = 0.0283$ ,  $\alpha_0 + \alpha_{p0}/\omega$  can be measured by sending the chopper timing signal into a time-of-flight histogram during fixed-phase operation. The phase sampling, which should be uniform to achieve the desired result, can be verified by histogramming source time origin pulses during random-phase operation. The analysis assumes that the detectors operate with time-independent efficiencies.

#### IV. CALCULATION OF DELAYED NEUTRON COUNTING RATE FROM THE MEASUREMENT

We now explore an iterative approach as an approximate method for determining the relationship of the delayed neutron counting rate to the prompt response. Integrating the expression for the prompt response (equation 8) with respect to wavelength  $\lambda$ , we obtain for either scattered neutron or beam monitor data

$$C_p(t) = [(1-\epsilon)/f] (h/md) F((h/m)t/d) P_c((h/m)t/d, L_c t/d - \alpha_0/\omega; 0). \quad (10)$$

The factor  $P_c$  represents the reduction of the observed intensity by the chopper, which may be only partially open. Substituting  $\lambda = (h/m)t/d$ , we obtain from equation (7) the following expression for  $F(\lambda)$ ,

$$F(\lambda) = [f/(1-\epsilon)] (md/h) C_p((m/h)\lambda d) / P_c(\lambda, L_c(m/h)\lambda - \alpha_0/\omega; 0). \quad (11)$$

We now substitute this expression into that for the delayed neutron response given by equation (8), and obtain

$$C_d(t) = \epsilon f / (1-\epsilon) \int dt' C_p(t') P_c((h/m)t'/d, t - (d-L_c)t'/d - \alpha_0/\omega; 0) / P_c((h/m)t'/d, L_c t'/d - \alpha_0/\omega; 0). \quad (12)$$

This result is exact, and in view of equation (10) the integral always converges, but is unfeasible if the  $t'$  integration includes the range where the denominator vanishes but the numerator does not. According to (10),  $C_p$  vanishes just when the denominator in (12) vanishes, so (12) is valid everywhere that it is of interest. Of course to produce the result (12), the prompt response  $C_p(t)$  must be measured, recorded and available throughout the range where it does not vanish. Figure 5 illustrates this range; there,  $\Delta t$  represents the range of times during which the chopper is open.

Since  $C_d$  is in some sense small compared to  $C_p(t)$ ,

$$C_d(t) \approx \epsilon f / (1-\epsilon) \int dt' C(t') P_c(0, t - (d-L_c)t'/d - \alpha_0/\omega; 0) / P_c(0, L_c t'/d - \alpha_0/\omega; 0), \quad (13)$$

Equation (13) suggests an iterative scheme to obtain the delayed neutron counting rate. The  $n^{\text{th}}$  iteration would give the delayed response  $C_{dn}(t)$  from the prompt response  $C_{pn}(t)$ . That is

$$C_{dn}(t) = \epsilon f / (1-\epsilon) \int dt' C_{pn}(t') P_c(0, t - (d-L_c)t'/d - \alpha_0/\omega; 0) / P_c(0, L_c t'/d - \alpha_0/\omega; 0). \quad (14)$$

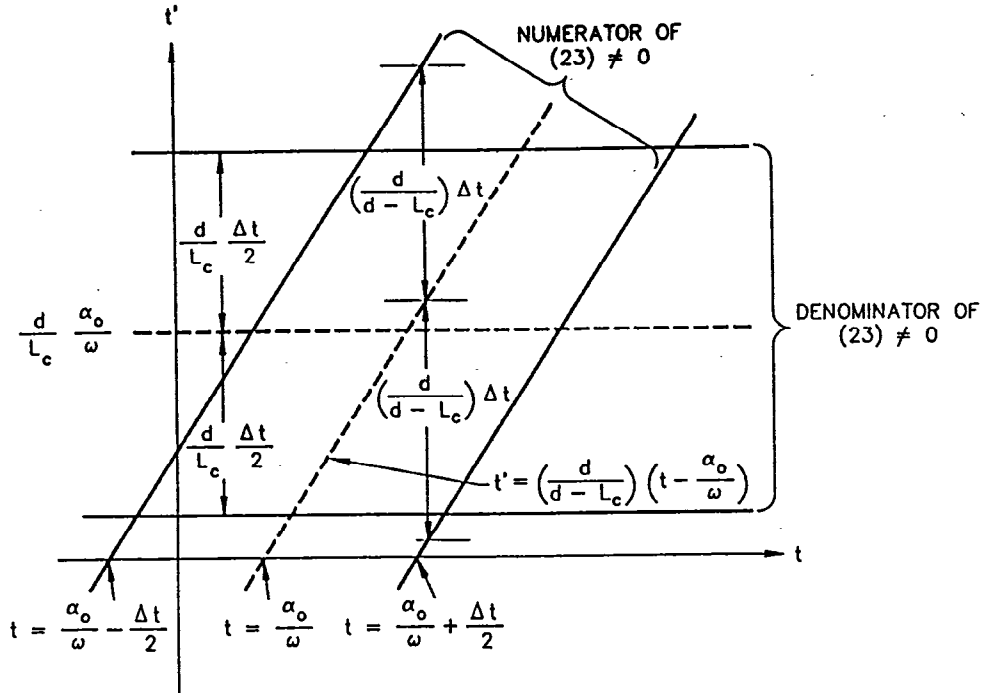


Figure 5. A schematic diagram in  $(t, t')$  space showing the region within which the chopper transmission probability  $P_c(\lambda, t; 0) \neq 0$ , where  $\lambda$  is the neutron wavelength,  $t'$  and  $t$  are the times when the neutron is at the moderator and at the detector respectively. The chopper rotates at angular speed  $\omega$ , and the initial phase angle  $\alpha_0$  is 0. The lines  $t' = (d/L_c)(\alpha_0/\omega \pm \Delta t/2)$  represent the boundaries of the region for which the denominator of (12) is non-zero, and the lines  $t' = d/(d-L_c)(t - \alpha_0/\omega \pm \Delta t/2)$  represent the boundaries of the region for which the numerator of (12) is non-zero, where  $\Delta t(\lambda)$  is the chopper open time.

This result is used to obtain the  $(n+1)^{\text{th}}$  value of the prompt response  $C_{pn+1}(t)$ . That is,

$$C_{pn+1}(t') = C(t') - C_{dn}(t'), \quad (15)$$

where  $C(t')$  is the counting rate of the measurement, and  $C_{dn}(t')$  is the  $n^{\text{th}}$  calculation of the correction to it due to delayed neutron background. For the initial calculation we take  $C_{d0}(t') = 0$ , or  $C_{p1}(t') = C(t')$ . Such a calculation can be checked against the exact random-phase chopper method of measuring the delayed neutron background. The procedure is a feasible basis for routine correction of scattered neutron and beam monitor data.

## V. MEASUREMENTS

We have measured the chopped, delayed neutron counting rate as a function of time in both the GPPD and SEPD diffractometers at IPNS. The source pulsing frequency for these measurements was 15 Hz rather than the usual 30 Hz, in order to provide data at long times when the counting rate due to prompt neutrons is low (this time interval corresponds normally to the "second frame" during normal 30 Hz operation). Delayed neutrons, which represent a fraction  $\epsilon=0.0283$  of the total (see equation (2)) then spread over a 66.7 msec interval rather than the normal 33.3 msec interval between pulses. Thus the ratio of the delayed neutron

counting rate to the prompt neutron counting rate is one-half the ratio for normal conditions.

Data were collected in three modes of operation: with the chopper rotating at 15 Hz, opening twice per revolution as during normal operation, and phased as during normal operation ( $\alpha_0/\omega = 6500 \mu\text{sec}$  for SEPD,  $4400 \mu\text{sec}$  for GPPD); with the chopper rotating at  $\sim 15$  Hz and asynchronous relative to the source; and with the chopper stopped open. A 6-mm diameter vanadium rod was placed in the sample position. Scattered neutron counting rates were recorded for all scattering angles with time focussing. During random-phase operation, timing signals from the accelerator were recorded which indicated uniform sampling of the source-chopper phase. The moderator was liquid  $\text{CH}_4$  at  $\sim 105\text{K}$ .

Figure 6 shows the counting rate for detectors at  $150^\circ$  scattering angle for SEPD, (a) with the chopper running and phased with the source, and (b) with the chopper stopped and open; the time origin is the time of the source pulse. Figure 6c shows the counting rate for the same detectors, with the chopper operating at random phase; the time origin is the time of the chopper reference pulse shifted by  $\alpha_0/\omega = 6500 \mu\text{sec}$ . The prompt response dominates the counting rate in the source-phased cases; the chopper has little effect on the prompt response in the interval  $0 < t < 30\text{msec}$ . The rise at short times is due to epithermal neutrons. The peak at 6 msec is due to the 130K Maxwellian. The  $\lambda$ -like discontinuities are polycrystalline Bragg edges due to aluminum in the neutron path. Between 30 and 50 msec is the peak due to the second opening of the chopper. The same peak occurs 33 msec earlier, but is small relative to the prompt pulse response. The shape of the delayed neutron counting rate is revealed in Fig. 6c, where, due to the random-phase operation, all neutrons appear to be coming from a steady source. The chopped, delayed neutron peak exactly corresponds to the 30-50 msec peak of Fig. 6a.

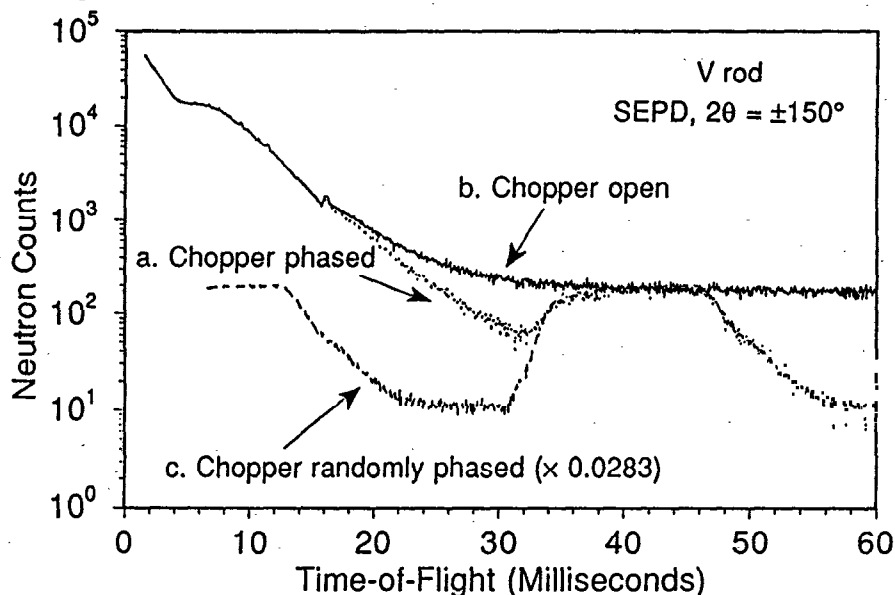


Figure 6. The scattered neutron counting rate from a vanadium rod sample in SEPD detectors at  $2\theta = 150^\circ$ , normalized to proton current; a) with the chopper running and in phase with the source, b) with the chopper stationary and open, and c) with the chopper operating at random phase relative to the source, normalized by  $\epsilon = 0.0283$  (eq. 9) and shifted by  $\alpha_0/\omega = 6500 \mu\text{sec}$ .



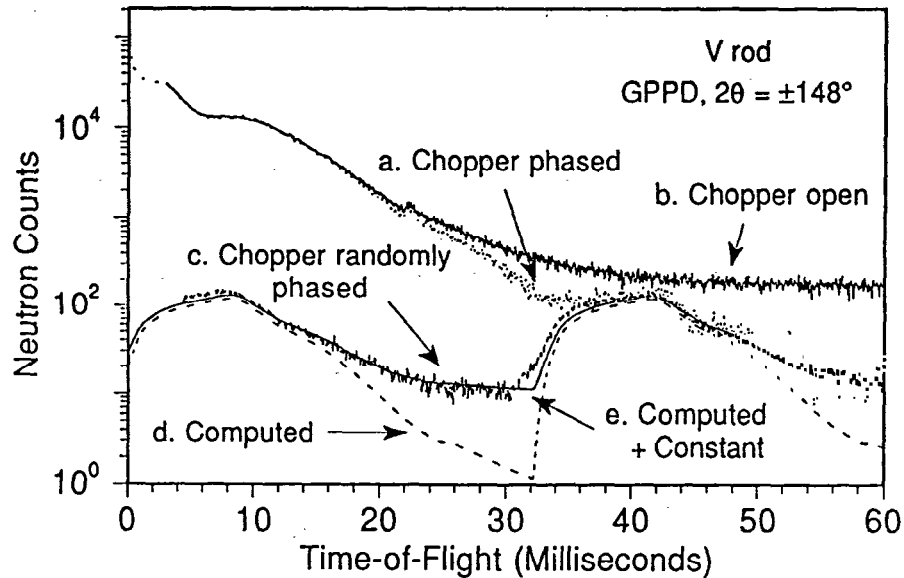


Figure 7. The scattered neutron counting rate from a vanadium rod sample in GPPD detectors at  $2\theta=148^\circ$ , normalized to proton current; a) with the chopper running and in phase with the source, b) with the chopper stationary and open, and c) with the chopper operating at random phase relative to the source, normalized by  $\epsilon=0.0283$  (eq. 9) and shifted by  $\alpha_0/\omega=4400 \mu\text{sec}$ . The delayed neutron counting rate computed from a) according to equations (14) and (15), d) without constant correction, e) with constant correction of 10 counts/channel.

Figure 7 shows (a) the chopper-phased, and (b) chopper-stopped-open data, for neutrons scattered by the 6 mm diameter vanadium rod into detectors at  $148^\circ$  scattering angle in GPPD; and Figure 7c shows the corresponding random-phase data. The random phase data are normalized according to equation (9), with  $f=15$  Hz,  $\omega/2\pi=15$  Hz, and  $\epsilon=0.0283$ <sup>(5)</sup>.

We have calculated the delayed neutron background for GPPD from the observed total counting rate distribution for the case of the chopper running and phased to the source, according to equations (14) and (15). The result converged after two iterations. Comparing the result to the random phase data we find a constant contribution of background in addition to the computed chopped background. We have estimated this constant background which is caused by very short wavelength neutrons. These can penetrate the boron carbide of the drum chopper since the black chopper approximation is invalid for short wavelength neutrons ( $E \gtrsim 65$  eV). This background added to the delayed neutron peak is also shown in Figure 7. The discrepancy of the leading edge with the data is caused primarily by the time-focusing of the detectors which results in a uniform smearing of functions of scattered neutron time-of-flight by  $\Delta t/t \sim 0.032$  for the GPPD diffractometer.

## VI. CONCLUSIONS

Expressions for the pulse shape (transmission probability) and open time functions of drum choppers developed previously<sup>3</sup> have been used for the calculation of the prompt and delayed neutron counting rates in pulsed source diffractometers. An exact method is suggested for determining the delayed neutron counting rate, using the prompt and delayed neutrons with the chopper

operating in random phase with respect to the source. In addition, we have examined three approximate methods by which the delayed neutron response might be determined in terms of the prompt response; these appeal to the calculated pulse shape functions and might be refined iteratively. These approximate methods might be checked using the exact random-phase chopper method. We also report measurements which confirm the analysis of this random-phase chopper method.

## VII. ACKNOWLEDGEMENTS

We thank James D. Jorgensen, R. Kent Crawford and Richard L. Hitterman for assistance in the planning and execution of the measurements, and Lawrence I. Donley and George E. Ostrowski for assistance in arranging the random phase operation of the chopper systems. This work was performed under the auspices of the U.S. Department of Energy, Division of Materials Sciences, Office of Basic Energy Sciences, under Contract W-31-109-ENG-38.

## VIII. REFERENCES

1. A. E. Knox, J. M. Carpenter, J. L. Bailey, R. J. Armani, R. N. Blomquist, B. S. Brown, D. R. Henley, A. G. Hins, B. A. Loomis, A. W. Schulke and H. R. Thresh, Proc. IXth Meeting of the International Collaboration on Advanced Neutron Sources (ICANS IX), Villigen, Switzerland, 1986. SIN report ISBN 3-907998-01-4 (July 1987) 557-591.
2. J. D. Jorgensen, J. Faber Jr., J. M. Carpenter, R. K. Crawford, J. R. Haumann, R. L. Hitterman, R. Kleb, G. E. Ostrowski, F. J. Rotella and T. G. Worlton, J. Appl. Cryst. 22 (1989), 321-333.
3. J. M. Carpenter and D. F. R. Mildner, "Transmission Probability of a Drum Chopper in a Thermal Neutron Beam". Submitted to Nucl. Instr. & Meth.
4. R. K. Crawford, J. E. Epperson, P. Thiyagarajan and J. M. Carpenter, these proceedings.
5. J. E. Epperson, J. M. Carpenter, P. Thiyagarajan, and B. Heuser, Nucl. Inst. & Meth. A289 (1990) 30-34.

The submitted manuscript has been authored by a contractor of the U. S. Government under contract No. W-31-109-ENG-38. Accordingly, the U. S. Government retains a nonexclusive, royalty-free license to publish or reproduce the published form of this contribution, or allow others to do so, for U. S. Government purposes.